AIP | Applied Physics Letters

Nanocrystalline Si/SiO2 core-shell network with intense white light emission fabricated by hot-wire chemical vapor deposition

Y. Matsumoto, A. Dutt, G. Santana-Rodríguez, J. Santoyo-Salazar, and M. Aceves-Mijares

Citation: Applied Physics Letters **106**, 171912 (2015); doi: 10.1063/1.4919527
View online: http://dx.doi.org/10.1063/1.4919527
View Table of Contents: http://scitation.aip.org/content/aip/journal/apl/106/17?ver=pdfcov
Published by the AIP Publishing

Nanocrystalline Si/SiO_2 core-shell network with intense white light emission fabricated by hot-wire chemical vapor deposition

Y. Matsumoto,[1,a),b)] A. Dutt,[1,b)] G. Santana-Rodríguez,[2] J. Santoyo-Salazar,[3] and M. Aceves-Mijares[4]
[1]*SEES, Electrical Engineering Department, Centro de Investigación y de Estudios Avanzados del Instituto Politécnico Nacional, Cinvestav-IPN, Mexico, D.F. 07360, Mexico*
[2]*Institute of Material Research, Universidad Nacional Autónoma de México, Coyoacán 04510, Mexico*
[3]*Department of Physics, Centro de Investigación y de Estudios Avanzados del Instituto Politécnico Nacional, Cinvestav-IPN, Mexico, D.F. 07360, Mexico*
[4]*Departament of Electronics, Instituto Nacional de Astrofísica Óptica y Electrónica, Tonantzintla, Puebla 72000, Mexico*

(Received 21 February 2015; accepted 20 April 2015; published online 30 April 2015)

We report the fabrication of a stable Si/SiO_2 core-shell network using hot-wire chemical vapor deposition on a silicon substrate at a relatively low substrate temperature of 200 °C. Structural investigations using transmission electron microscopy and X-ray diffraction confirm the presence of nanocrystalline silicon and silicon dioxide quantum dots in the form of a core-shell network embedded in the amorphous SiO_x matrix, while selected area electron diffraction confirms the formation of a core-shell structure. The core-shell structure exhibits a bright white emission that can be seen with the unaided eye at room temperature without any post-annealing treatments, and the observed photoemission does not alter in color or intensity after prolonged laser exposure. Additional measurements are performed while varying the laser power and optical gain is found in the as-deposited material. Intense stable white luminescence is observed and shows the prospective for various optical and biological applications in the future. © *2015 AIP Publishing LLC*.
[http://dx.doi.org/10.1063/1.4919527]

Attaining Si-based visible or white light emission is one of the challenging goals for optoelectronic device fabrication, and abundant research has been done to expand the horizons of Si thin films for optical applications.[1–3] White luminescence from Si quantum dots can be used in bright solid state lighting with the additional benefit of low energy consumption. Currently, white light-emitting device structures consist of a blue InGaN light-emitting diode with a yellow phosphor coating, but this material has the constraint of color quenching with changing temperature.[4,5] Therefore, it is important to replace the current materials with Si technology, which possesses the additional advantages of increased safety, simpler process, and a more stable material. In previous research, some groups have illustrated a wavelength-tunable optical response related to the quantum confinement effect in silicon-based nanocrystals.[6,7] Furthermore, other groups have observed that the optical properties do not only depend upon the nanoparticles themselves, but also the dielectric matrix surrounding the particles. The interface between the silicon/silicon oxide matrices is a frequently studied issue because of its technological importance and the interesting photoluminescence-related mechanisms.[8] Other reports also exist related to the visible emission and tunable nature of the photoluminescence (PL) of silica-covered silicon nanoparticles.[9,10] In many of the processes, PL was observed after high-temperature treatments that formed nanoparticles inside the matrix (nc-Si/SiO_2), which is a process that is not favorable for industrial mass production. For this reason, research on the fabrication of low-temperature deposited silicon nanoparticles embedded in an amorphous matrix has been performed.[11,12] Nanoparticles with core-shell structures are highly advanced materials which have the advantage that their properties can be tailored to a greater extent than exists with their single component nanoparticle counterparts. When the shell consists of a material resembling SiO_2, it is especially important in the resulting physical characteristics because the nanoparticles are more stable owing to the chemically inert nature of the shell, and the shape and size of the nanoparticle can be controlled by the thickness and spatial distribution of the shell.[13] There have been a number of reports related to the formation of core-shell nanoparticles using chemical synthesis for diverse applications,[14–18] and one recent report has explained the luminescence mechanism in the near infrared region as it relates to the core-shell structure.[15] However, the realization of visible or white PL from as-deposited core-shell samples is still an uninvestigated topic.

In this Letter, transmission electron microscopy (TEM), X-ray diffraction (XRD), and selected area electron diffraction (SAED) are used to demonstrate the formation of an Si/SiO_2-based core-shell network, prepared by means of the hot-wire chemical vapor deposition (HW-CVD) method at a low substrate temperature of 200 °C, where the sample exhibits a bright white emission. The HW-CVD system is a recently emerged technique that, among other techniques, has the advantages of an efficient use of gases and the absence of plasma (ion) damage during the thin film deposition process. During the deposition process, source gases such as

[a)]Author to whom correspondence should be addressed. Electronic mail: ymatsumo@cinvestav.mx
[b)]Y. Matsumoto and A. Dutt contributed equally to this work.

silane (SiH_4), oxygen (O_2), and hydrogen (H_2) were decomposed in the growth chamber with the help of a catalyst to produce various radical species and to assist in the growth of the thin film.[11] The formation of the core-shell network using HW-CVD in the present work supports the results of previous simulation work from other groups investigating the same materials,[8,19–21] and supports the theoretical aspects with the experimental data. Moreover, using power variation PL analysis, evidence of a possible optical gain was found for this material, which demonstrates its potential importance in the silicon-based optical device industry. In addition, HW-CVD fabrication can more easily be integrated into industry-level production than other fabrication processes.[22]

The HW-CVD system employed for the depositions has been described elsewhere.[12] In the present work, a tantalum (Ta) wire 0.5 mm in diameter was used as the catalyst material and the distance between filament and substrate was kept constant at 5 cm. Two types of substrate materials were used, including Corning glass 2497C and p-type crystalline silicon. The initial background pressure in the chamber was maintained at 10^6 Torr using a turbo-molecular pump, and the filament temperature (T_{fil}) was kept at 1800 °C, while the substrate temperature T_{subs} was maintained at 200 °C. The flow rate was maintained at 5 sccm for the pure silane SiH_4 and hydrogen gases, whereas oxygen was maintained at 0.5 sccm for 10, 20, and 40 min of deposition. The amorphous-to-crystalline phase transitions were analyzed using X-ray diffraction (Siemens D5000), and the PL spectra were obtained at room temperature using a He-Cd laser (Kimmon Koha Co., Ltd., Centennial, CO, USA) with an excitation wavelength of 325 nm and a varying output power of 3.5–15.5 mW. The Si/SiO_2 core-shell network was detected experimentally with XRD and simulated by considering the Wyckoff positions in the Diamond Software 3.0.[23] Bright field images and SAED were obtained in a TEM (JEOL-JEM-2010) at 200 kV with a wavelength of 0.027 Å and a camera distance of 20 cm.

Figure 1(a) shows the structural representation of the Si/SiO_2 derived from experimental data and using the Diamond Software, which considers the growth mechanism of the core-shell network in three feasible evolution steps. The silicon Wyckoff positions are given as one atom of Si (1) at the 8*a* (0, 0, 0) site (-43*m*) and the other atom of Si (2) at the 16*c* (0.125, 0.125, 0.125) site (-3*m*), where the silicon structure has a density of 6.99026 g/cm^3 and a lattice parameter $a = 5.4301$ Å in the cubic space group *Fd*-3*m* No. 227. The silicon has preferential growth at [111] according to XRD and high-resolution TEM characterizations. The silicon dioxide (SiO_2) Wyckoff positions are given as the Si atom at the 8*a* (0, 0, 0) site (-43*m*) and the oxygen (O) atom at the 16*c* (0.125, 0.125, 0.125) site (-3*m*), where the SiO_2 structure has a density of 2.17438 g/cm^3 and a lattice parameter $a = 7.1600$ Å in the cubic space group *Fd*-3*m* No. 227. However, it is possible to find a distortion in the SiO_2 from a cubic to a hexagonal structure, where the SiO_2 shell can crystallize to the hexagonal symmetry class P3121, with lattice constants $a = 4.9138$ Å and $c = 5.4052$ Å and a density of 2.65000 g/cm^3. The core-shell formation illustrated in Fig. 1(a) indicates (I) the assembling of the Si/SiO_2 network structure where the network endeavors to accumulate in the states with a minimum bonding affinity energy. In this case, the SiO_2 shell initially clusters around the Si core at 10 min. (II) With the course of processing time and in the presence of the surface temperature, the SiO_2 dot begins to achieve stability around the Si core network at 20 min. (III) The formation of a stable Si/SiO_2 core-shell network with preferential growth at [533] and [111] over the Si surface is seen at 40 min. Dong *et al.* have studied this type of configuration using density-functional tight-binding calculations, and according to the prescribed model, the gap energy of the Si/SiO_2 core-shell network is a competition between the quantum confinement and the oxidation effects depending upon the size of the Si core.[21] Additionally, this model illustrates the theoretical explanation of the tunable PL in the Si/SiO_2 core-shell structure. Figure 1(b) shows the X-ray diffractogram of samples obtained as a function of the deposition time, where peaks corresponding to silicon (111), (220), and (311) can be observed in all three of the diffraction patterns.[24] At the same time, diffraction patterns for the samples

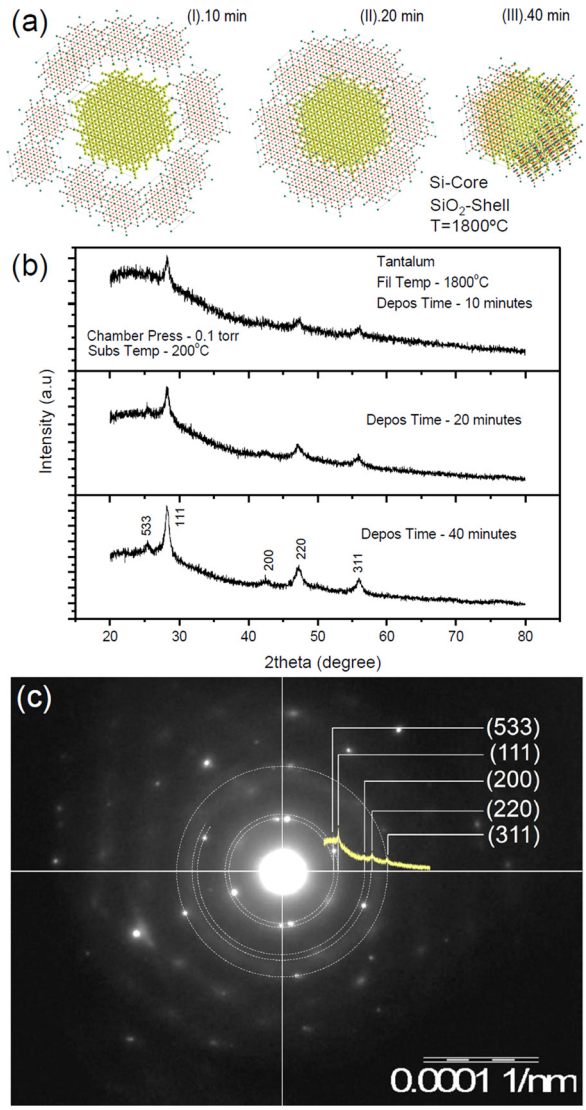

FIG. 1. Si/SiO_2 core-shell structures: (a) Representation of growth evolution for Si/SiO_2 core-shell network at (I) 10 min, (II) 20 min, and (III) 40 min by diamond software of the thin film deposited; (b) crystallization changes were observed by XRD spectra from the thin film deposited at $T_{sub} = 200$ °C and $T_{fil} = 1800$ °C; and (c) SAED pattern for one of the crystalline regions at $T_{sub} = 200$ °C and $T_{fil} = 1800$ °C for 20 min of deposition.

deposited at 20 and 40 min exhibit two extra peaks at the 2θ values of 25.44° and 42.44° where, in the literature, these two peaks correspond to the cubic and hexagonal phases of silicon dioxide, respectively.[25,26] This observation confirms the presence of both silicon and silicon dioxide crystalline phases in the film. However, the stable well-formed Si/SiO_2 core-shell assembly induces some small structural changes in the lattice owing to inter-phase bonding and, as a consequence, the plane related to the cubic phase of SiO_2 (533) has a corresponding change in position from 24.07° to 25.44°.

The SAED patterns related to the nc-Si/SiO_2 structures are shown in Fig. 1(c), where the diffraction patterns exhibit points and diffused rings owing to the formation of the core-shell structure. In the SAED, hexagonal rings corresponding to SiO_2 (200) in the outer part of the image can be seen, which verifies the hypothesis made from the XRD results concerning the presence of SiO_2 particles along with Si phases. The distance between the hexagonal rings corresponds to the interatomic distances *d*, *h*, *k*, and *l*, and the diffracted planes of the silicon and silicon oxide structure are displayed at the same positions. To authenticate the presence of nc-SiO_2 particles, TEM measurements are carried out for the samples with 20 and 40 min of deposition time (Figs. 2(a) and 2(b), respectively). The TEM images show crystallites of different nanometric sizes surrounded by an amorphous environment, and in accordance with the simulation demonstrated in Fig. 1(a), it can be observed that the smaller particles seen to form the cluster structure begin to lose their free energy and to rearrange themselves in equilibrium form. After 20 min of deposition time, particles can be found at isolated locations (Fig. 2(a)), whereas the sample after 40 min of deposition exhibits the cluster structure of Si and SiO_2 nanoparticles (Fig. 2(b)), which is in agreement with Fig. 1(a) (III). Crystal planes in these images are identified as belonging to {533} and {111} with different orientations and the interatomic distance at (533) changed from 3.69 to 3.75 Å on average. With the help of the TEM images, the whole process can be observed as the formation of nc-Si nuclei followed by the formation of crystallite-promoted silicon-oxide as a shell as a result of the catalytic reaction from the used precursors. For this reason, it is supposed that the entire network takes the stable core-shell form of silicon and silicon oxide. The thickness of the corresponding shell structure is found to be 4.33 nm and that of the core assembly nearby to be 21 nm.

Figure 3(a) shows the room-temperature PL spectra of the sample as a function of varying pump power for the laser excitation source, where the power is varied from 3.5 to 15.5 mW with a 1.5 mW step size. As can be seen, a whole PL spectrum can be observed for the entire visible region (400–700 nm). The influence of the laser power upon the integrated PL intensity is shown in the top right inset of Fig. 3(a), and the PL spot corresponding to the white emission, which is able to be seen with the naked eye in a dark room, is shown in the second inset of Fig. 3(a). Generally, the white broad PL spectra could be considered the contribution of well-known silicon defects in the red (1.9 eV), green (2.35 eV), and blue (2.8 eV) bands or it could be owing to a wide distribution of various small-sized nanoparticles. The red band generally arises from defects known as nonbridging oxygen hole centers,[27] while the green band has been attributed to hydrogen bonding-related species in the thin film possessing composites of SiO_2 nanoparticles.[28] Even surface trapped excitons give rise to PL spectra between 2 and 3 eV.[29]

In the current study, a wide distribution of 2–4-nm-diameter nc-Si/SiO_2 particles can be observed (Fig. 2(a)) whose calculated band gap is in the range of 1.5–2.5 eV using the relation[30] $Epl = Eg + (3.73/d^{1.39})$, where Eg is the band gap of bulk silicon and *d* is the average diameter of the nanocrystals. Figure 3(b) shows the resulting band diagram with the probable recombination energy levels related to the size of the nanoparticles, as well as bands linked to the known defects from nonbridging oxygen hole centers, surface trapped excitons, and Si–H, where it is believed that

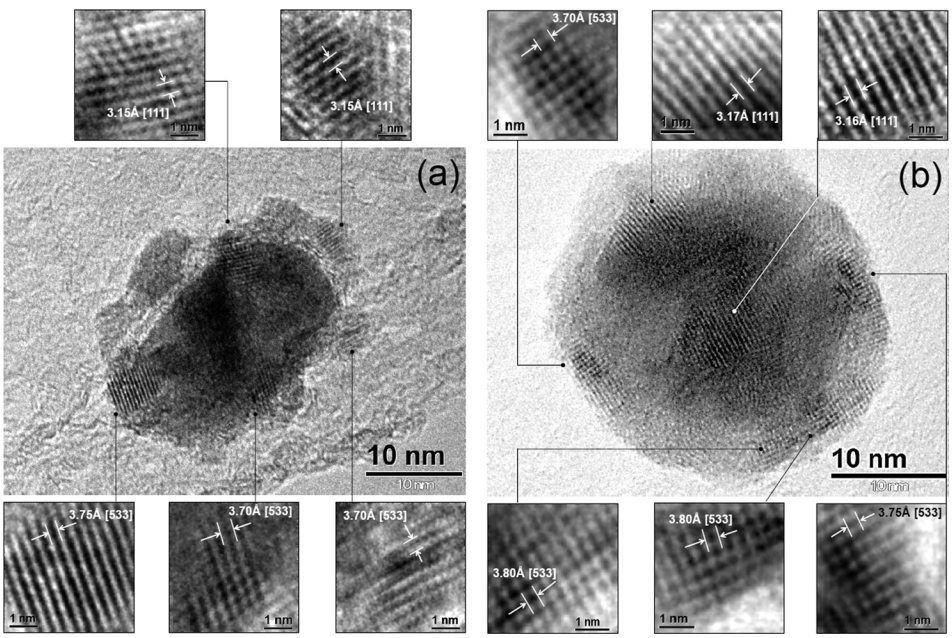

FIG. 2. TEM images form Si/SiO_2 core shell. (a) Cross sectional TEM image showing a region with Si/SiO_2 nano-crystals of various sizes and orientations; (b) TEM images shows the core-shell nature of nc-Si/SiO_2 particles in the SiO_x matrix at crystalline regions at $T_{sub} = 200\,°C$ and $T_{fil} = 1800\,°C$ for 20 min of deposition. Inset: the {533} and {111} can be observed in both cases.

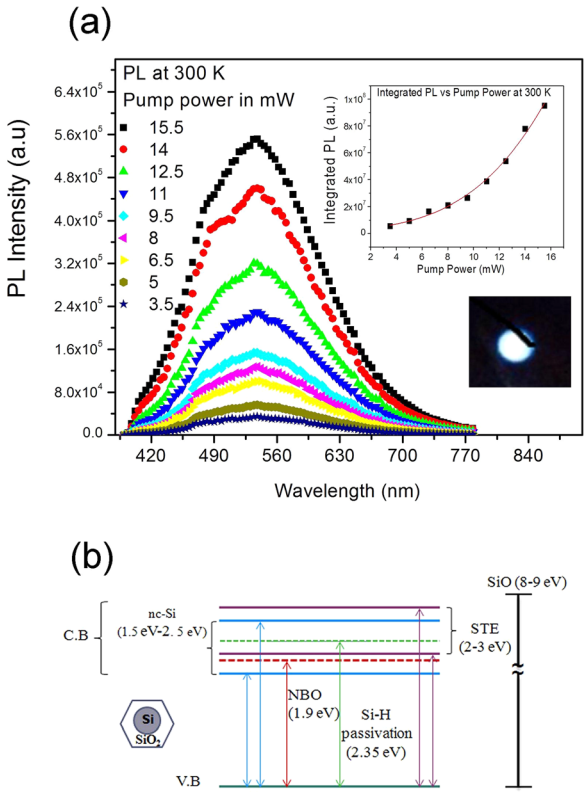

FIG. 3. Luminescence and energy levels related to Si/SiO_2 core shells: (a) PL spectra of as-deposited film at $T_{sub} = 200\,^{\circ}C$ and $T_{fil} = 1800\,^{\circ}C$ with respect to laser power from 3.5 mW to 15.5 mW, with the inset on the top right side showing the spectra corresponding to integrated intensity as a function of laser power, whereas the other inset corresponds to the white luminescence; (b) Energy levels corresponding to the defects states and to the trap levels related to the band gap of quantum dot's associated to nc-Si/SiO_2 in the amorphous matrix.

radiative emission occurs upon electron transitions between these different established levels. Because the different energy levels are so close to each other, this produces uncertainty about the exact roles of the confinement effect or the defects in the observed white luminescence. In the present study, samples were excited with a He-Cd laser (3.8 eV), which was enough to excite the core-shell network of nc-Si/SiO_2, though it could likewise excite some of the defects illustrated in Fig. 3(b). The kind of response observed in Fig. 3(a) inset, however, effectively eliminates the role of interface states or defects in the observed PL because the present laser excitation energy can only excite the electron-hole pairs inside the nanoparticles by the progressive filling of the conduction and the valence bands. Moreover, the exponential increase of the integrated luminescence is shown to be a function of the laser power, which exhibits a tendency to optical gain in these types of materials.[31] By increasing the photon number, e.g., by increasing the pump power, there could be a situation wherein the integrated PL intensity of the nanocrystals decreases as more nonradiative levels related to surface and other defects states become easily accessible.[32] Nevertheless, in this case, the increase in the integrated PL intensity signifies the confinement-related nature of the emission. An additional benefit of the SiO_2 shell is that it comprises a Si = O double bond at the Si/SiO_2 interface, which is a particularly good bond for the passivation of dangling bonds.[6] Ultimately, all of the passivation and confinement from the nano-sized core-shell particles leads to the stable white emission from this structure. This stable and low-cost material could be useful for optical device fabrication of light emitting devices as well as for *in vivo* biological analysis owing to the fine emission and nontoxic nature of the silicon nanoparticles.[16]

In summary, the formation of a low-temperature deposited core-shell structure of nc-Si/SiO_2 was demonstrated using HW-CVD with an intense white PL response at room temperature without any post-deposition treatments. The TEM images and SAED patterns confirmed the presence of a stable core-shell network, and white emission was ascribed to the quantum confinement effect inside the well-passivated silicon nanoparticles. In future, this material could be used for the fabrication of optical devices based on the optical gain obtained from this structure.

The authors thank Angela Gabriela López for sample preparations. The authors are indebted to Adolfo Tavira Fuentes and Marcela Guerrero for their technical assistance. We would express our sincere thanks to Ing Miguel Ángel Avendaño Ibarra for his technical support. This project was supported by the National Council of Science and Technology (CONACyT) Nos. CB2009-128723 and CB2012-179632. The authors also acknowledge financial support from CONACYT-SENER under Contract No. 151076.

[1]R. J. Walters, G. I. Bourianoff, and H. A. Atwater, Nat. Mater. **4**, 143 (2005).
[2]M. Zacharias, J. Heitmann, R. Scholz, U. Kahler, M. Schmidt, and J. Bläsing, Appl. Phys. Lett. **80**, 661 (2002).
[3]P. Cuony, D. T. L. Alexander, I. Perez-Wurfl, M. Despeisse, G. Bugnon, M. Boccard, T. Söderström, A. Hessler-Wyser, C. Hébert, and C. Ballif, Adv. Mater. **24**, 1182 (2012).
[4]R. S. Berns, *Billmeyer and Saltzman's Principles of Color Technology*, 3rd ed. (Wiley, New York, 2000).
[5]E. Jang, S. Jun, H. Jang, J. Lim, B. Kim, and Y. Kim, Adv. Mater. **22**, 3076 (2010).
[6]M. V. Wolkin, J. Jorne, P. M. Fauchet, G. Allan, and C. Delerue, Phys. Rev. Lett. **82**(1), 197 (1999).
[7]Y. Li, B. Qian, Z. Sui, and C. Jiang, Appl. Phys. Lett. **103**, 161908 (2013).
[8]N. Daldosso, M. Luppi, S. Ossicini, E. Degoli, R. Magri, G. Dalba, P. Fornasini, R. Grisenti, F. Rocca, L. Pavesi, S. Boninelli, F. Priolo, C. Spinella, and F. Iacona, Phys. Rev. B **68**, 085327 (2003).
[9]S. W. Lin and D. H. Chen, Small **5**(1), 72 (2009).
[10]Z. Kang, Y. Liu, C. H. A. Tsang, D. D. D. Ma, X. Fan, N. B. Wong, and S. T. Lee, Adv. Mater. **21**(6), 661 (2009).
[11]Y. Matsumoto, M. A. Reyes, and A. Escobosa, J. Appl. Phys. **98**, 014909 (2005).
[12]Y. Matsumoto, S. Godavarthi, M. Ortega, V. Sánchez, S. Velumani, and P. S. Mallick, Thin Solid Films **519**, 4498 (2011).
[13]F. Caruso, Adv. Mater. **13**, 11 (2001).
[14]C. M. Hessel, M. R. Rasch, J. L. Hueso, B. W. Goodfellow, V. A. Akhavan, P. Puvanakrishnan, J. W. Tunnel, and B. A. Korgel, Small **6**, 2026 (2010).
[15]J. Joo, J. F. Cruz, S. Vijayakumar, J. Grondek, and M. J. Sailor, Adv. Funct. Mater. **24**, 5688 (2014).
[16]J. H. Park, L. Gu, G. von Maltzahn, E. Ruoslahti, S. N. Bhatia, and M. J. Sailor, Nat. Mater. **8**, 331 (2009).
[17]D. Tan, B. Liu, D. Chen, and G. Shen, RSC. Adv. **4**, 18391 (2014).
[18]J. Niu, S. Zhang, Y. Niu, R. Song, H. Song, X. Chen, J. Zhou, and S. Hong, RSC. Adv. **4**, 29435 (2014).
[19]M. Luppi and S. Ossicini, Phys. Status Solidi A **197**(1), 251 (2003).
[20]Z. Zhou, L. Brus, and R. Friesner, Nano Lett. **3**(2), 163 (2003).
[21]H. Dong, T. Hou, X. Sun, Y. Li, and S. Tong Lee, Appl. Phys. Lett. **103**, 123115 (2013).
[22]H. Matsumura and K. Ohdaira, Thin Solid Films **516**, 537 (2008).

[23]W. T. Pennington, J. Appl. Crystallogr. **32**, 1028 (1999).
[24]H. E. Swanson and R. K. Fuyat, Natl. Bur. Stand. Circ. **539**(II), 6 (1953).
[25]H. E. Swanson and R. K. Fuyat, Natl. Bur. Stand. Circ. **539**, 3 (1953).
[26]V. Fülop, G. Borbely, H. K. Beyer, S. Ernst, and J. Weitkamp, J. Chem. Soc., Faraday Trans. 1 **85**, 2127 (1989).
[27]G. Pacchioni, L. Skuja, and D. L. Griscom, *Defects in SiO_2 and Related Dielectrics Science and Technology* (Springer, 2000), p. 73.
[28]Yu. D. Glinka, S. H. Lin, and Y.-T. Chen, Appl. Phys. Lett. **75**, 778 (1999).
[29]C. Itoh, K. Tanimura, and N. Itoh, J. Phys. C: Solid State Phys. **21**, 4693 (1988).
[30]C. Delerue, G. Allan, and M. Lannoo, Phys. Rev. B **48**, 11024 (1993).
[31]L. Pavesi, L. Dal Negro, C. Mazzoleni, G. Franzo, and F. Priolo, Nature **408**, 440 (2000).
[32]D. Timmerman, J. Valenta, K. Dohnalova, W. D. A. M. de Boer, and T. Gregorkiewicz, Nat. Nanotechnol. **6**, 710 (2011).